

Thermal Physics and Statistical Mechanics Driven Inertial Confinement Fusion (ICF) Inducing a Controlled Thermonuclear Energy

Bahman Zohuri^{1,2}, Farahnaz Behgounia¹ and Masoud J. Moghaddam²

1. Golden Gate University, Ageno School of Business, San Francisco, California 94105, USA

2. Galaxy Advanced Engineering, Albuquerque, New Mexico 87111, USA

Abstract: In the 1970s, scientists began experimenting with powerful laser beams to compress and heat the hydrogen isotopes to the point of fusion, a technique called ICF (Inertial Confinement Fusion). In the “direct drive” approach to ICF, powerful beams of laser light are focused on a small spherical pellet containing micrograms of deuterium and tritium. The rapid heating caused by the laser “driver” makes the outer layer of the target explode. In keeping with Isaac Newton’s Third Law “For every action, there is an equal and opposite reaction”, the remaining portion of the target is driven inwards in a rocket-like implosion, causing compression of the fuel inside the capsule and the formation of a shock wave, which further heats the fuel in the very center and results in a self-sustaining burn. The fusion burn propagates outward through the cooler, outer regions of the capsule much more rapidly than the capsule can expand. Instead of magnetic fields, the plasma is confined by the inertia of its own mass—hence the term inertial confinement fusion. A similar process can be observed on an astrophysical scale in stars and the terrestrial uber world, that have exhausted their nuclear fuel, hence inertially or gravitationally collapsing and generating a supernova explosion, where the results can easily be converted to induction of energy in control forms for a peaceful purpose (i.e., inertial fusion reaction) by means of thermal physics and statistical mechanics behavior of an ideal Fermi gas, utilizing Fermi-Degeneracy and Thomas-Fermi theory. The fundamental understanding of thermal physics and statistical mechanics enables us to have a better understanding of Fermi-Degeneracy as well as Thomas-Fermi theory of ideal gas, which results in laser compressing matter to a super high density for purpose of producing thermonuclear energy in way of controlled form for peaceful shape and form i.e. CTR (Controlled Thermonuclear Reaction). In this short review, we have concentrated on Fundamental of State Equations by driving them as it was evaluated in book *Statistical Mechanics* written by Mayer, J. and Mayer, M. in this article.

Key words: renewable, nonrenewable source of energy, fusion reactors, super high density matter, laser driven fusion energy, Fermi-Degeneracy, Thomas-Fermi theory, return on investment, total cost of ownership.

1. Introduction

NIF (National Ignition Facility), located at LLNL (Lawrence Livermore National Laboratory), will be the first laser in which the energy released from the fusion fuel will equal or exceed the laser energy used to produce the fusion reaction—a condition known as ignition. Unlocking the stored energy of atomic nuclei will produce ten to 100 times the amount of energy required to initiate the self-sustaining fusion burn. Creating ICF (Inertial Confinement Fusion) and energy

gain in the NIF target chamber will be a significant step toward making fusion energy viable in commercial power plants. LLNL scientists also are exploring other approaches to developing ICF as a commercially viable energy source, a process that is considered as FI (Fast Ignition) [1].

FI is the approach, which is being taken by the NIF to achieve thermonuclear ignition, and burn is called the “central hot spot” scenario. This technique relies on simultaneous compression and ignition of a spherical fuel capsule in an implosion, roughly like in a diesel engine. Although the hot-spot approach has a high probability of success, there also is considerable

Corresponding author: Bahman Zohuri, Ph.D., adjunct professor, artificial intelligence and machine learning.

interest in a modified approach called FI, in which compression is separated from the ignition phase. FI uses the same hardware as the hot-spot approach but adds a high-intensity, ultra-short-pulse laser to provide the “spark” that initiates ignition. A deuterium-tritium target is first compressed to high density by lasers, and then the short-pulse laser beam delivers energy to ignite the compressed core—analogueous to a sparkplug in an internal combustion engine [1].

Moreover, to accommodate the symmetry conditions needed, the absorption of laser energy must be carefully determined starting from the early stages [7, 8]. The absorption data for dense plasmas are also required for fast ignition by ultra-intense lasers due to creation of plasmas by the nanosecond pre-pulse [9]. Least understood are laser-plasma interactions that involve strongly coupled $\Gamma > 1$ and partially degenerate electrons. Such conditions also occur in warm dense matter experiments [10, 11] and laser cluster interactions [1].

To explain the apparent fluid-like behavior of the current filamentation instability in FI scenarios, many experts in the field of ICF have developed analytical theory for the coupling of electromagnetic instabilities to electrostatic modes. This theory shows that as cold electrons tend to filament at a faster rate than hot ones they pull with them the ions. Because hot electrons are usually in the minority, the filaments of the bulk of the electron population overlap with those of the ions, which is exactly what one would have expected from a fluid instability (such as Rayleigh-Taylor). Nevertheless, this is a purely kinetic electromagnetic phenomenon. The predicted growth rate was confirmed using Particle-In-Cell simulations and the physics is illustrated in Fig. 1.

The analytical theory was only available for beam-like distributions, such as drifting Gaussian and water bag distribution. However, in order to overcome this problem and to resolve this, one can calculate the stability properties (growth/damping rate) of electromagnetic modes for arbitrary electron distribution functions.

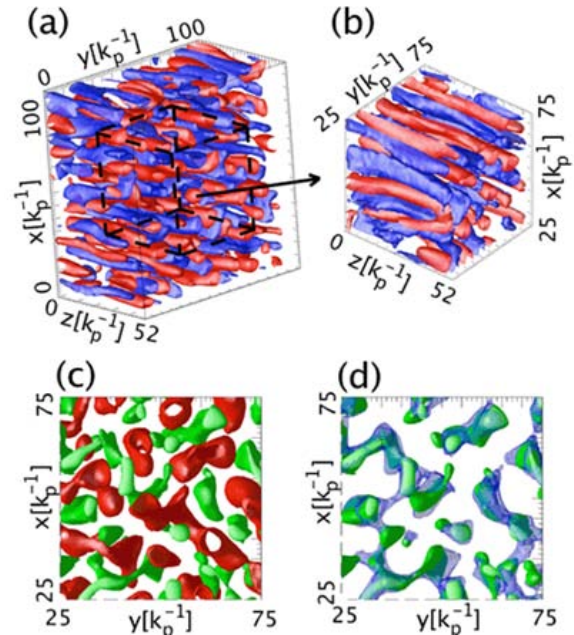


Fig. 1 Filamentation of counter-streaming electron beams (red/blue density isosurfaces) leads to filamentation of the background ions (green isosurfaces). The colder (blue) electron filaments attract the ions [1].

Because modern thermonuclear weapons use the fusion reaction to generate their immense energy, scientists will use NIF ignition experiments to examine the conditions associated with the inner workings of nuclear weapons.

Ignitions experiments also can be used to help scientists better understand the hot, dense interiors of large planets, stars and other astrophysical phenomena.

Here in this short review, we consider an elementary account of thermal physics. The subject is simple, the methods are powerful, and the results have broad applications. Probably no other physical theory is used more widely throughout science and engineering. In order to study of plasma physics and its behavior for a source of driving fusion for a controlled thermonuclear reaction for purpose of generating energy, in particular using high power laser or particle beam source, requires an understanding of the fundamental knowledge of thermal physics and statistical mechanics theory as part of essential education. As part of this education, we need to have a better concept of the EOS (Equation of State) for ideal gases, which proves to be

the central to the development of early molecular and atomic physics. In our case, it will lay down the ground for laser or high-energy particle beam compression of matter to super-high densities as [1, 2]:

1. Thermonuclear applications, an event that in nature, takes place at extraterrestrial in stars and
2. Surface of the sun and terrestrially in a nuclear explosion.

Nuckolls, et al. [2] in their published paper in 1972 under the title of “Laser Compression of Matter to Super-high Densities: Thermonuclear (CTR) Applications” established the ground based on their initial research at LLNL, that hydrogen may be compressed to more than 10,000 times liquid density by an implosion system energized by a high energy laser [2].

This scheme makes possible efficient thermonuclear burn of small pellets of heavy hydrogen isotopes and feasible fusion power reactors using practical lasers.

The implosion process to a focal point first was solved numerically by Guderley [3] utilizing the application of self-similarity of the second kind for deducing a closed solution in one-dimensional form [3-6].

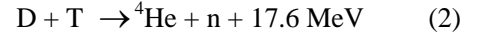
For a thermonuclear burning to take place in extra-terrestrially in stars as well as in a nuclear explosion, we need to look at a specific thermonuclear burn rate that is proportional to density and is given by Eq. (1).

$$\frac{\partial \rho}{\partial t} \sim \rho \overline{\sigma v} \quad (1)$$

where $\partial \rho / \partial t$ is the fractional burnup, ρ is the density, and $\overline{\sigma v}$ is the Maxwell velocity-average reaction cross-section. With this relationship being satisfied, except at high fuel of let say D-T (e.g. Deuterium (D) and Tritium (T), the two isotopes of Hydrogen (H) element) depletions, the thermonuclear energy production at a fixed ion temperature is proportional to the Lawson number [7] ($n \times \tau$), a product of density n and confinement time τ .

In case of D-T reaction of Eq. (2) in MCF (Magnetic

Confinement Fusion) for purpose of CTR (Controlled Thermonuclear Reaction),



The Lawson number, also known as Lawson criterion, is defined as illustrated in Eq. (3).

$$n \tau \geq 10^4 \text{ s/cm}^3 \quad (3)$$

where in this case, n is the plasma density in units of particles per cm^3 and τ is the time in seconds for which the plasma τ of density n is going to be confined.

However, in case of ICF, the same Lawson criterion of Eq. (3) shapes in different form as $\rho r \geq 1 \text{ gram/cm}^2$, where ρ and r are the compressed fuel density and radius pellet, respectively. In order, for the confinement criteria also known as Lawson criterion to be satisfied, it needs to take place, before the occurrence of Rayleigh-Taylor hydrodynamics instability would happen for uniform illumination of the target's surface, namely pellet of Deuterium and Tritium. See Section 3.4 of Ref. [1] written by Zohuri for further information.

Note that: in conventional CTR approaches, the density is limited by material properties, and the objective is to achieve sufficiently long confinement times by the use of electromagnetic fields [8].

In the case of laser driven pellet fuel of D-T reaction to induce a controlled fusion energy (i.e. ICF), the main objective is to achieve a breakeven by satisfying Lawson criterion (i.e. at the minimum amount of laser energy in needs to be equal to the minimum fusion of energy out). For this matter to be achieved, a sufficient high fuel density needs to take place, while the confinement time is determined by the inertia of matter.

“Spherical compression of 10^4 fold via the laser implosion scheme described here reduces the laser energy required for CTR by more than one thousand-fold, from more than 10^8 - 10^9 Jules, which is so large as to be currently impractical to 10^5 - 10^6 Jules, assuming laser and thermal/electric efficiencies of 10%

and 40% respectively” [2].

“Note that one kJ of laser energy may be sufficient to generate an equal thermonuclear energy” [2].

2. Implosion Driven by Laser Compression of Fuel Pellet

In nature, hydrogen in the center of the sun is believed to exist at more than one thousand times liquid density, and at pressures greater than 10^{11} atmospheres (temperature $\sim 1-2$ keV) [9].

These pressures are maintained gravitationally by the overlying enormous solar mass, $\sim 10^{33}$ grams. Matter in the cores of white dwarf stars is believed to exist at more than 10^5 gram/cm³, and at pressures greater than 10^{15} atmospheres [10].

Moreover, we would be able to have a gripe of the situation by having a better understanding of the behavior of electron in white cores that are obeying Fermi-Degenerate, so the pressure is a minimum determined by the quantum mechanical uncertainty principles [11] and for hydrogen with Fermi-Degenerate electrons is given by the Eq. (4) [12].

$$P = \frac{2}{3} n_e \varepsilon_F \left[\frac{3}{5} + \frac{\pi^2}{4} \left(\frac{kT}{\varepsilon_F} \right)^2 - \frac{3\pi^4}{80} \left(\frac{kT}{\varepsilon_F} \right)^4 + \dots \right] \quad (4)$$

In this short review here, our task would be to derive this equation for an ideal Fermi gas, first by defining it, secondly via thermal physics utilizing statistical mechanics come to the conclusion of ICF generating CRT that is driven by Fermi energy of Eq. (5) via pressure given in Eq. (4).

$$\varepsilon_F = \frac{h^2}{8m} \left(\frac{3}{\pi} n_e \right)^{2/3} \quad (5)$$

where n_e is the electron density, kT is the thermal energy, $h = 6.62607004 \times 10^{-34}$ m² kg/s, and m is the electron mass. At 10^4 times liquid density ($n_e = 5 \times 10^{26}$), the minimum hydrogen pressure occurs, when $kT \ll \varepsilon_F$, and is approximately 10^{12} atmospheres.

This is the way that we can reproduce the thermal energy on earth similar to what we observe at the sun surface as well as other terrestrial stars.

Bear in mind that electron degeneracy pressure [13] is a particular manifestation of the more general phenomenon of quantum degeneracy [14] pressure. In quantum mechanics, an energy level is degenerate if it corresponds to two or more different measurable state of quantum system as illustrated in Fig. 2.

Conversely, two or more different states of a quantum mechanical system are said to be degenerate if they give the same value of energy upon measurement. The number of different states corresponding to a particular energy level is known as the degree of degeneracy of the level. It is represented mathematically by the Hamiltonian for the system having more than one linearly independent eigenstate with the same energy eigenvalue.

Note that degeneracy plays a fundamental role in quantum statistical mechanics.

Also, from the knowledge of our quantum mechanics and quantum energy state, we know that, per Pauli exclusion principle, we are disallowed by having two identical half-integer spin particles (electrons and all other fermions) from simultaneously occupying the same quantum state. The result is an emergent pressure against compression of matter into smaller volumes of space. The principle and fundamental aspect of

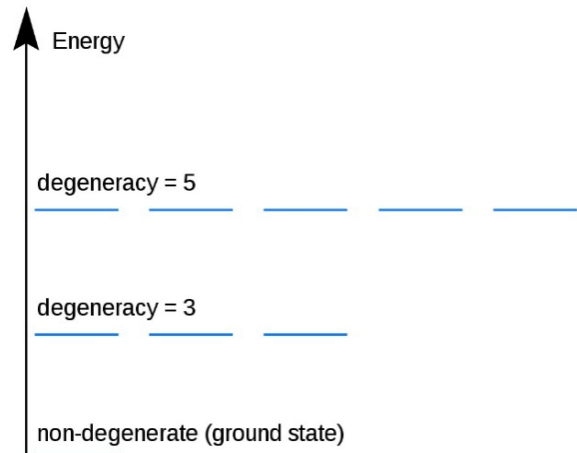


Fig. 2 Degenerate states in a quantum system [14].

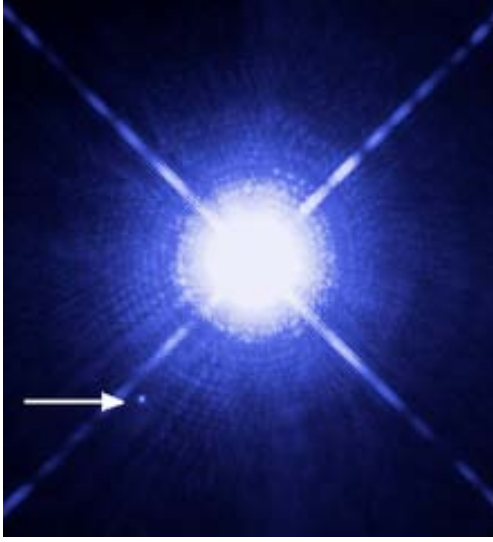


Fig. 3 Image of white dwarfs Sirius A and B [18].

compressing pellet fueled by D-T to a FI steps driving ICF.

For bulk matter with no net electric charge, the attraction between electrons and nuclei exceeds (at any scale) the mutual repulsion of electrons plus the mutual repulsion of nuclei; so absent electron degeneracy pressure, the matter would collapse into a single nucleus.

In 1967, Freeman Dyson showed that solid matter is stabilized by quantum degeneracy pressure rather than electrostatic repulsion [15-17].

Because of this, electron degeneracy creates a barrier to the gravitational collapse of dying stars and is responsible for the formation of white dwarfs as illustrated in Fig. 3, an image of Sirius A and B taken by the Hubble Space Telescope [18]

Sirius B, which is a white dwarf, can be seen as a faint point of light to the lower left of the much brighter Sirius A [18].

3. Ideal Fermi Gas

To describe and define an ideal Fermi gas, we may state that it is strongly determined by the Pauli principle by considering the limit as presented in Eq. (6) here, which defines the degenerate Fermi gas as:

$$\mu \gg k_B T \Leftrightarrow \beta \mu \gg 1 \quad (6)$$

which defines the degenerate Fermi gas and this equation $\beta = 1/k_B T$ is the inverse temperature, and T is the temperature and k_B is the Boltzmann constant.

Note that β is called thermodynamic beta in the field of statistical thermodynamics subject, which is also known as coldness, is the reciprocal of the thermodynamic temperature of a system as defined above. In Eq. (6), the parameter μ is representing the total chemical potential (Fermi level) of the three-dimensional ideal Fermi gas is related to the zero temperature Fermi energy ε_F of Eq. (5) by a Sommerfeld expansion, where we are assuming $k_B T \ll \varepsilon_F$:

$$\mu(T) = \varepsilon_0 + \varepsilon_F \left[1 - \frac{\pi^2}{12} \left(\frac{k_B T}{\varepsilon_F} \right)^2 - \frac{\pi^4}{80} \left(\frac{k_B T}{\varepsilon_F} \right)^4 + \dots \right] \quad (7)$$

Hence, the internal chemical potential $\mu - \varepsilon_0$ is approximately equal to the Fermi energy at temperatures that are much lower than the characteristic Fermi temperature T_F . This characteristic temperature is on the order of 10^5 K for a metal, hence at room temperature (300 K), the Fermi energy and internal chemical potential are essentially equivalent.

In the limit, defined by Eq. (6), the quantum mechanical nature of the system becomes especially important, and the system has little to do with the classical ideal gas.

Furthermore, electrons are part of a family of particles known as fermions. Fermions, like the proton or the neutron, follow Pauli's principle and Fermi-Dirac statistics. In general, for an ensemble of non-interacting fermions, also known as Fermi gas, each particle can be treated independently with a single-fermion energy given by the purely kinetic term ε , presented in Eq. (8) as:

$$\varepsilon = \frac{p^2}{2m} \quad (8)$$

where p is the momentum of one particle and m is

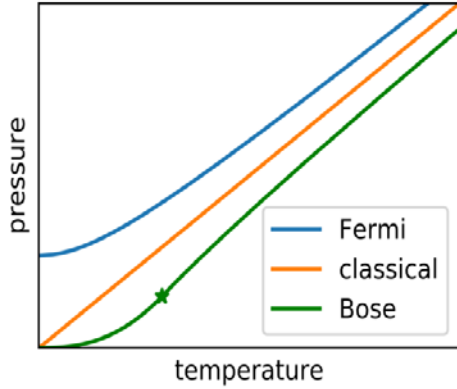


Fig. 4 Pressure vs. temperature.

its mass. Every possible momentum state of an electron within this volume up to the Fermi momentum p_F is being occupied.

Fig. 4 is the pressure vs temperature curves of classical and quantum ideal gases (Fermi gas, Bose gas) in three dimensions. Pauli repulsion in fermions (such as electrons) gives them an additional pressure over an equivalent classical gas, most significantly at low temperature.

Moreover, the degeneracy pressure at zero temperature can be computed as [19]:

$$P = \frac{2}{3} \frac{E_{Total}}{V} = \frac{2}{3} \frac{p_F^2}{10\pi^2 m \hbar^3} \quad (9)$$

where V is the total volume of the system and E_{Total} is the total energy of the ensemble. Specifically for the electron degeneracy pressure, m is substituted by the electron mass m_e and the Fermi momentum is obtained from the Fermi energy, so the electron degeneracy pressure is given by Eq. (10) as:

$$P_e = \frac{(3\pi^2)^{2/3} \hbar^2}{5m_e} \rho_e^{5/3} \quad (10)$$

where ρ_e is the free electron density (the number of free electrons per unit volume). For the case of a metal, one can prove that this equation remains approximately true for temperatures lower than the Fermi temperature, about 10^6 Kelvin.

When particle energies reach relativistic levels, a modified formula is required. The relativistic

degeneracy pressure is proportional to $\rho_e^{4/3}$.

Note that again, in white dwarfs, electron degeneracy pressure will halt the gravitational collapse of a star if its mass is below the Chandrasekhar limit (1.44 solar masses) and presented by Eq. (11) [20]:

$$M_{Limit} = \frac{\omega_3^0 \sqrt{3\pi} \left(\frac{\hbar c}{G} \right)^{3/2}}{2} \frac{1}{(\mu_e m_H)^2} \quad \text{Eq. (11)}$$

where:

- $\hbar = \frac{h}{\pi}$ is the reduced Plank constant;
- c is the speed of light;
- G is the gravitational constant;
- μ_e is the average molecular weight per electron,

which depends upon the chemical composition of the star;

- m_H is the mass of the hydrogen atom;
- $\omega_3^0 \approx 2.018236$ is a constant connected with the solution to the Lane-Emden equation;

• $m_p = \sqrt{\frac{\hbar c}{G}}$ is the Plank mass, the limit is the order of M_{plimit}^3 / m_H^2 .

The limiting mass can be obtained formally from the Chandrasekhar's white dwarf equation by taking the limit of large central density.

A more accurate value of the limit than that given by this simple model requires adjusting for various factors, including electrostatic interactions between the electrons and nuclei and effects caused by nonzero temperature [21].

Lieb and Yau [22] have given a rigorous derivation of the limit from a relativistic many-particle Schrödinger equation.

This is the pressure that prevents a white dwarf star from collapsing. A star exceeding this limit and without significant thermally generated pressure will continue to collapse to form either a neutron star or black hole, because the degeneracy pressure provided by the electrons is weaker than the inward pull of gravity.

Note that in the non-relativistic case, electron degeneracy pressure gives rise to an EOS of the form $P = K_1 \rho^{5/3}$, where P is the pressure, ρ is the mass density, and K_1 is a constant.

Solving the hydrostatic equation leads to a model white dwarf that is a polytropic of index $3/2$ – and therefore has radius inversely proportional to the cube root of its mass, and volume inversely proportional to its mass [23].

As the mass of a model white dwarf increases, the typical energies to which degeneracy pressure forces the electrons are no longer negligible relative to their rest masses. The velocities of the electrons approach the speed of light, and special relativity must be taken into account. In the strongly relativistic limit, the EOS takes the form $P = K_2 \rho^{4/3}$. This yields a polytropic of index 3, which has a total mass, M_{limit} say, depending only on K_2 [23].

For a fully relativistic treatment, the EOS used interpolates between the equations $P = K_1 \rho^{5/3}$ for small ρ and $P = K_2 \rho^{4/3}$ for large ρ . When this is done, the model radius still decreases with mass, but becomes zero at M_{limit} . This is the Chandrasekhar limit [23].

The curves of radius against mass for the non-relativistic and relativistic models are shown in Fig. 5. They are colored blue and green, respectively. μ_e has been set equal to 2. Radius is measured in standard solar radii or kilometers, and mass in standard solar masses [24].

Fig. 4 shows radius-mass relations for a model white dwarf.

The green curve uses the general pressure law for an ideal Fermi gas, while the blue curve is for a non-relativistic ideal Fermi gas. The black line marks the ultra-relativistic limit.

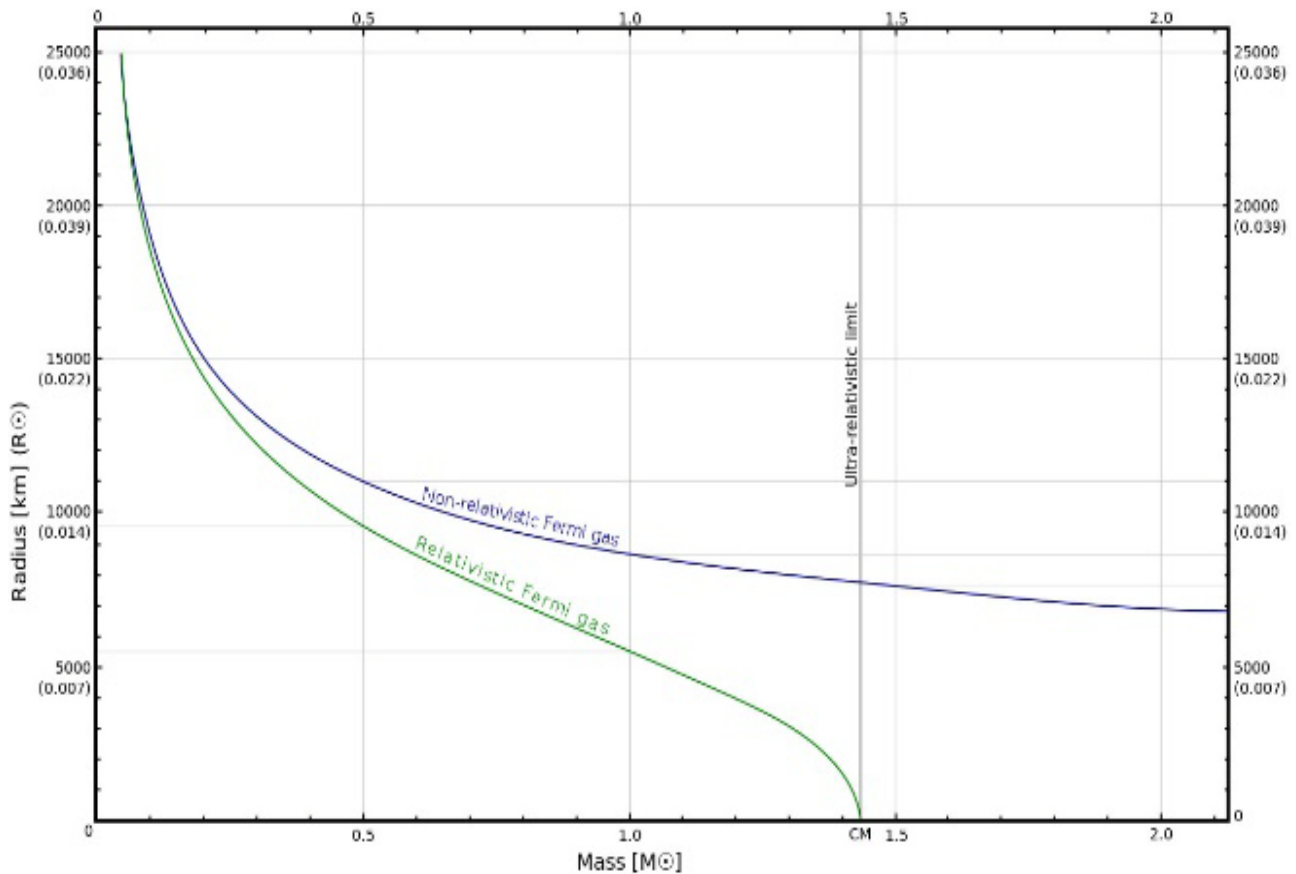


Fig. 5 Radius-mass relations for a model white dwarf.

(Source: www.wikipedia.org)

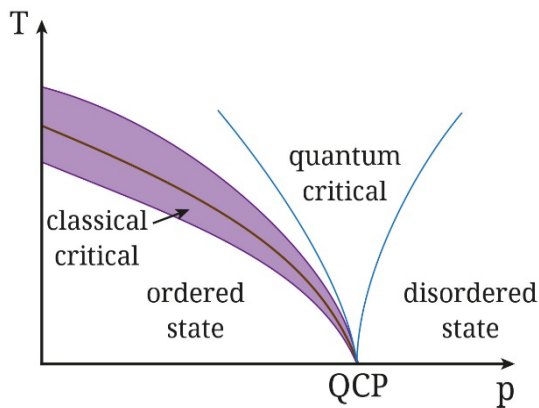


Fig. 6 Phase diagram of a second order quantum phase transition.

(Source: www.wikipedia.org)

As a lump sum of this section, we may state that an ideal Fermi gas is a state of matter which is an ensemble of many non-interacting fermions. Fermions are particles that obey Fermi-Dirac statistics, like electrons, protons, and neutrons, and, in general, particles with half-integer spin. These statistics determine the energy distribution of fermions in a Fermi gas in thermal equilibrium, and are characterized by their number density, temperature, and the set of available energy states, as illustrated in Fig. 6.

The model is named after the Italian physicist Enrico Fermi [25].

This physical model can be accurately applied to many systems with many fermions. Some key examples are the behavior of charge carriers in a metal, nucleons in an atomic nucleus, neutrons in a neutron star, and electrons in a white dwarf.

4. Fundamentals of EOS

The EOS gives an impressive demonstration of how great a fraction of the inorganic world is explained by the revolutionary deviation from classical mechanics to quantum mechanics. At the same time, the EOS presents the tools by which our experimental knowledge can be extended into regions of extreme concentrations of energy and matter.

In a very holistic definition way, the EOS describes a physical system by the relation between its

thermodynamic quantities, such as pressure, energy, density, entropy, specific heat, etc., and is related to both fundamental physics and the applied sciences. Important branches of physics were developed or originated from the equations of state, while in return more complex formulations of the EOS were due to the development of modern physics.

For super-fast moving objects, Einstein extended classical mechanics to what we know as the theory of relativity by revolutionizing a new era for quantum mechanics and Planck-Bohr-Heisenberg-Schrodinger for very small objects, thermodynamics and statistics were developed to describe EOS of matter in extreme density and temperature domains.

Later on, the EOS of high pressure was studied experimentally in a laboratory by using static and dynamic techniques driven by a sample being squeezed between pistons or anvils and the pressure and temperature are limited by the strength of the construction materials for a few megabars and a few hundred degrees of Celsius. This is the approach that the scientists and physicists working in the field of ICF are taking, by pressing the ablation surface of the fuel pellet of D-T adiabatically, so the corona of the pellet containing two hydrogen isotopes of Deuterium (D) and Tritium (T) reaches a FI level for fusion purpose.

Bear in mind that in the dynamic experiments shock waves can be created by means of the Hugoniot relationship, driven by measuring the shock wave parameters, such as shock wave speed and particle flow velocity. The EOS are studying the fluid equations of motions, where the state of a moving fluid or gas can be defined in terms of its velocity, density, and pressure as functions of a position, and time. These functions are obtained by integral equations or differential equations which are derived from the conservation laws of mass, momentum and energy [26].

In conclusion, since the passage time of the shock is short in comparison to the disassembly time of the shocked medium, one can study EOS for any pressure that can be supplied by the source of driver.

5. Degenerate Gases

By definition in a simple form, we can state that a degenerate gas is the type of gas in which, because of high density, the particle concentration is so high that the Maxwell-Boltzmann distribution does not apply, and the behavior of the gas is governed by quantum statistics.

Examples of degenerate gases are the conduction of electrons in a metal, the electrons in a white dwarf, and the neutrons in a neutron star.

With high density concentration within the nature of degenerate gas, comes degeneracy pressure, and briefly, we may state that the pressure in a degenerate gas of fermions caused by the Pauli exclusion principle and the Heisenberg uncertainty principle. Because of the exclusion principle, fermions at a high density, with small interparticle spacing, must have different momenta; from the uncertainty principle, the momentum difference must be inversely proportional to the spacing. Consequently, in a high-density gas (small spacing) the particles have high relative momenta, which leads to a degeneracy pressure much greater than the thermal pressure.

Furthermore, stars are supported by the degeneracy pressure of the electron gas in their interior, which is obeying Eq. (1) formulation. Degeneracy pressure is the increased resistance exerted by electrons composing the gas, as a result of contraction of stellar, as we expressed at the beginning of this article. The application of the so-called Fermi-Dirac statistic and of special relativity to the study of the equilibrium structure of white dwarf stars (see Fig. 7) leads to the existence of a mass-radius relationship through which a unique radius is assigned to a white dwarf of a given mass; the larger the mass, the smaller the radius.

White dwarfs and neutron stars are supported against collapse under their own gravitational fields by the degeneracy pressure of electrons and neutrons, respectively.

To put what just stated in general perspective, the degenerate gas, in physics is a particular configuration,

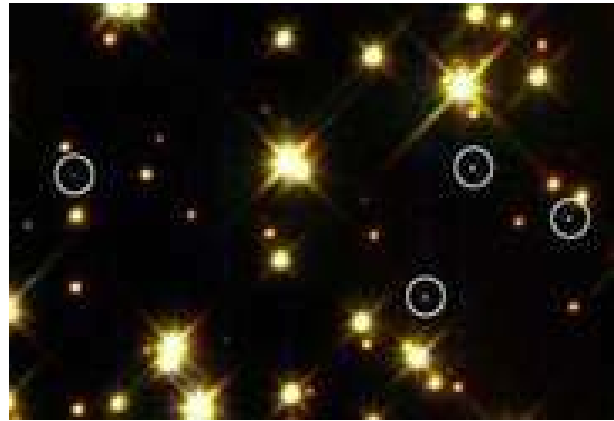


Fig. 7 White dwarf stars.

(Source: www.wikipedia.org)

which usually reached at high densities of a gas composed of subatomic particles with half-integral intrinsic angular momentum (i.e. spin).

Such particles are called fermions, because their microscopic behavior is regulated by a set of quantum mechanical rules—Fermi-Dirac statistics.

These rules state, in particular, that there can be only one fermion occupying each quantum-mechanical state of a system. As particle density is increased, the additional fermions are forced to occupy states of higher and higher energy, because the lower-energy states have all been progressively filled. This process of gradually filling in the higher-energy states increases the pressure of the fermion gas, termed degeneracy pressure. A fermion gas in which all the energy states below a critical value (designated Fermi energy) are filled is called a fully degenerate, or zero-temperature, fermion gas. Such particles as electrons, protons, neutrons and neutrinos are all fermions and obey Fermi-Dirac statistics. The electron gas in ordinary metals and in the interior of white dwarf stars constitutes two examples of a degenerate electron gas.

Note that: Fermion, any member of a group of subatomic particles having odd half-integral angular momentum (spin $1/2, 3/2, \dots$), named for the Fermi-Dirac statistics that describe its behavior. Fermions include particles in the class of leptons (e.g., electrons, muons), baryons (e.g., neutrons, protons, lambda particles), and

nuclei of odd mass number (e.g. tritium, helium-3, uranium-233).

Fermions obey the Pauli exclusion principle, which forbids more than one particle of this type from occupying a single quantum state as illustrated in Fig. 2. This condition underlies, for example, the buildup of electrons within an atom in successive orbitals around the nucleus and thereby prevents matter from collapsing to an extremely dense state. Fermions are produced and undergo annihilation in particle-antiparticle pairs.

From Quantum Mechanical Distribution Function point of view, for the number of molecules per quantum cell, one can derive Eq. (12) as [12]:

$$\frac{N_j}{C_j} = \frac{1}{e^{\alpha + \varepsilon_j/kT} \mp 1} \quad (12)$$

In the above relation parameter of N , it denotes the number of particles, which at equilibrium, are found in a region j consisting of C_j cells, or quantum states of one particle, the energies of which lie between ε_j and $\varepsilon_j + \Delta\varepsilon_j$. The parameter α is determined by the condition that the total number N of particles in the system is fixed and that is $\sum_j N_j$, summed over all regions j , must be equal to N number of particles or the relation as presented in Eq. (13) [12].

$$\sum_j N_j = N \quad \text{Eq. (13)}$$

In Eq. (12), the parameter k is considered as Boltzmann constant, while T is temperature in Kelvin.

Note that Eq. (12) is applicable to all systems composed of mechanically independent particles. The minus (-) sign in Eq. (12) is to be used if the particles have symmetric eigenfunctions, in which case they are said to obey Bose-Einstein statistics. While, the plus (+) sign must be used if the particles have antisymmetric eigenfunctions, in which case they are said to obey Fermi-Dirac statistics. [1, 12]

In case of treating a perfect gas, the distribution

function of Eq. (12) is always modified by omitting the unity in the denominator. The difference between the two kinds of system disappears and classical or Boltzmann statistics is obtained. This approximation can certainly be made if e^α is large, or $N_j/C_j \ll 1$ for all regions j . The parameter α can be determined for monatomic gases by setting $\sum_j N_j = N$, with neglect of the unity in the denominator. The result is presented in Eq. (14) [12] here as:

$$e^\alpha = g \left(\frac{2\pi mkT}{h^2} \right)^{3/2} \frac{V}{N} = 0.026g \frac{M^{3/2} T^{5/2}}{P_{Atm}} \quad (14)$$

This is found to justify, a posteriori, the neglect that was introduced in Ref. [12].

The parameters in Eq. (14) are defined and given as:

M = the atomic weight;

g = the multiplicity of the ground level in one atom;

V = molar volume of the gas.

More details that are beyond scope of this short review article can be found in the book by Mayer and Mayer [12].

Bear in mind that, the Fermi-Dirac gas at zero temperature in case of metals especially their electrical conductivity, may be rather satisfactorily explained by assuming that metals contain a perfect gas of electron.

If each metal atom contributes one or as many electrons as its valency, to the electron gas, the density of particles in the gas is very high. The molar volume V of the electron gas is the atomic volume of the metal divided by a small integer. Note that the atomic volumes of metals are of the order of 10 cc.

Under this condition, the electrons obey Fermi-Dirac statistics and therefore, the distribution function of Eq. (12) is given in Eq. (15):

$$\frac{N_j}{C_j} = \frac{1}{e^{(\varepsilon_j - \mu)/kT} + 1} \quad (15)$$

The classical distribution function is that in which

the unity in the denominator of this equation is omitted [12].

Note that, the lowest energy of classical or a Bose-Einstein gas at $T = 0$ and ε_0 by taking the Fig. 1 into consideration, at the zero temperature all particles crowded into the lowest state and lose all kinetic energy.

For a Fermi-Dirac gas, this is not a possible case and the particles, in this case, are subject to the Pauli exclusion principle. This principle indicates that no more than one particle may be in one quantum state, or cell. Considering, these circumstances, the lowest energy of the gas of N particles, is therefore, obtained if the N cells of lowest energy are filled with one particle in each. The energy ε_0 of the gas at $T = 0$ is therefore different from zero and one can easily calculate the quantity of this energy.

The number of quantum states, $C(\varepsilon)\Delta\varepsilon$ of one particle, the energy of which lies between ε and $\varepsilon + \Delta\varepsilon$, is given by Eqs. (16) and (17) consequently as [12]:

$$C(\varepsilon)\Delta\varepsilon = 4\pi g \frac{mV}{h^3} (2m\varepsilon)^{1/2} \Delta\varepsilon \quad (16)$$

and

$$C(\varepsilon)\Delta\varepsilon = 2\pi g V \left(\frac{2m}{h^2} \right)^{3/2} \varepsilon^{1/2} \Delta\varepsilon \quad (17)$$

where m denotes the mass of the particle and V is the total volume, as well as g representing the degeneracy of the internal ground level of the particles.

Thus, for electrons with $g = 2$, owing to the two possible orientations of the spin, Eq. (17) reduces to the Eq. (18):

$$C(\varepsilon) = 4\pi V \left(\frac{2m}{h^2} \right)^{3/2} \varepsilon^{1/2} \quad (18)$$

With above result, we now can determine the number of cells with energy less or equal to μ_0 (i.e. $\varepsilon = \mu_0$, the chemical potential at ground zero) is given by Eq. (19) as:

$$\begin{aligned} \int_0^{\mu_0} C(\varepsilon) d\varepsilon &= 4\pi V \left(\frac{2m}{h^2} \right)^{3/2} \int_0^{\mu_0} \varepsilon^{1/2} d\varepsilon \\ &= \frac{8\pi}{3} V \left(\frac{2m\mu_0}{h^2} \right)^{3/2} \end{aligned} \quad (19)$$

Since this number must be equal to a number of particles or electrons N in the system, one can obtain the result as Eq. (20) as:

$$N = \frac{8\pi}{3} V \left(\frac{2m\mu_0}{h^2} \right)^{3/2} \quad (20)$$

And in term of μ_0 explicitly, we can obtain Eq. (21) as:

$$\mu_0 = \frac{h^2}{8m} \left(\frac{3N}{\pi V} \right)^{2/3} \quad (21)$$

Note that: the quantity μ_0 , which is the uppermost energy of the cells, frequently is called the Fermi energy.

Substituting Eqs. (20) and (21) into Eq. (18), we obtain another result for $C(\varepsilon)$ as Eq. (22):

$$C(\varepsilon) = \frac{3}{2} N \frac{\varepsilon^{1/2}}{\mu_0^{3/2}} \quad (22)$$

Looking at Eq. (22), it easily can be noted that we define a cell by both the translational quantum numbers, k_x, k_y, k_z and the internal quantum numbers of particle, which in this case consist of the two spin directions. One sometimes defines a cell by the translational quantum numbers only and says that two electrons of opposite spin may occupy this cell, which is in alignment with Pauli excursion principle. The difference, obviously, is one of nomenclature only.

Going forward, we can now express the total energy of the N particles in this distribution, namely, the energy ε_0 of the Fermi gas at $T_0 = 0$, is given by Eq. (23) as:

$$\varepsilon_0 = \int_0^{\mu_0} \varepsilon C(\varepsilon) d\varepsilon \quad (23)$$

Now utilizing Eqs. (21) and (22) and then integrating the result, leads to Eq. (24) as:

$$\varepsilon_0 = \frac{3}{5} N \mu_0 = \frac{3h^2}{40m} N \left(\frac{3N}{\pi V} \right)^{2/3} \quad (24)$$

The average energy per electron in the Fermi gas at $T_0 = 0$ is $3/5$ of that of the energetically highest particle or $3/5$ of the Fermi energy μ_0 .

Furthermore, the energy μ_0 depends inversely on the mass of particles by inserting for m the mass of the electron.

For molar volume $V \approx 10$ for most metals, it is seen that the Fermi energy of an electron gas is extremely high and in the next sections, we would show that thermodynamic properties of the gas above $T = 0$ can be obtained as a power series in kT/μ_0 as it is shown in Eq. (7). A series of that type must be expected to converge very rapidly, so that the behavior of the electron gas at room temperature is not greatly different from that at $T = 0$.

The Eq. (21) shows that both the small mass and the high density of the electron gas favor this high value of μ_0 .

Obviously, atoms or molecules have masses more than two thousand times that of an electron, so that the value of μ_0 for a chemical Fermi-Dirac gas, even at the same density, is very much smaller. With respect to all these above debates, a development with respect to kT/μ_0 for a chemical gas obeying the Pauli principle would lead to a series which converges at very low temperatures only, and at room temperature the thermodynamic functions are radically different from those at $T = 0$ which is discussed in Mayer and Mayer [12] chapters 5 through 8 and we encourage the reader to refer to this reference for more details that is beyond the scope of this short review.

However, note that the same results could be obtained for the electron gas at $T = 0$ using the distribution function as it is given in Eq. (15). In Eq. (15), the quantity $\mu(T)$ is a function of temperature T and would be determined by the condition that the total number of particles should be fixed.

Furthermore, at zero temperature ($T = 0$)

distribution function driven by Eq. (15) is zero if $\varepsilon_j > \mu(0)$ and it would be equal to 1 if $\varepsilon_j < \mu(0)$.

Moreover, the distribution function of Eq. (15) under above conditions represents the state that all cells with energy lower than $\mu(0)$ are filled and all the cells with higher energy would be empty.

What remains is the case, when $\varepsilon_j = \varepsilon = \mu(0)$. With this condition in hand, we encounter the situation that the distribution function has a discontinuity, as it suddenly drops from unity to zero. In this case, the Fermi energy μ_0 of the filled level of highest energy is equal to the value μ that is taking place in the distribution function provided by Eq. (15) at zero temperature or $T = 0$.

But in Chapter 6 of Ref. [12], it is shown that in general the quantity μ in Eq. (15) is the chemical potential which is $1/N$ times the free energy F , thus the free energy of the electron gas at $T = 0$ is $F_0 = N\mu_0$ and easily can be verified by direct calculation of the various thermodynamic functions at $T = 0$ and at a temperature above zero, the distribution temperature of Eq. (15) must be used for the evolution of thermodynamic functions as well [12].

6. Fermi-Dirac Gas Integrals Equations

In order to derive such a relationship, we can take the number of electrons $N(\varepsilon) \Delta\varepsilon$ into account for the energy ranging between ε and $\varepsilon + \Delta\varepsilon$ by driving it as a function of the temperature and volume by taking Eq. (18) and substituting $C(\varepsilon)$ into Eq. (15), then we obtain the number of electrons per cell as Eq. (25) here:

$$N(\varepsilon) = 4\pi V \left(\frac{2m}{h^2} \right)^{3/2} \frac{\varepsilon^{1/2}}{e^{(\varepsilon-\mu)/kT} + 1} \quad (25)$$

Now using Eq. (22), we also can find another form of Eq. (25), which is presented here as Eq. (26):

$$N(\varepsilon) = \frac{3N}{2\mu_0^{3/2}} \frac{\varepsilon^{1/2}}{e^{(\varepsilon-\mu)/kT} + 1} \quad (26)$$

in which μ_0 , defined by Eq. (21), is the chemical

potential at $T = 0$ and μ the potential at the temperature in question.

The integration of Eq. (25) over all values of ε serves to derive the value of μ as a function of temperature by equating the result the left-hand side of an integrated form of Eq. (26), mainly $\int_0^\infty N(\varepsilon)d\varepsilon$ to the total number of particles N .

Analyzing Eq. (26), one can realize that for $N(\varepsilon)$, μ will necessarily result as a function of μ_0 and kT alone. Furthermore, the energy may be determined from Eq. (27) as:

$$E = \int_0^\infty \varepsilon N(\varepsilon)d\varepsilon \quad (27)$$

In order to be able to integrate any form of the equation such as Eq. (27), we need to deal with the problem of making integration of the type:

$$I = \int_0^\infty f(\varepsilon)g(\varepsilon)d\varepsilon \quad (28)$$

where the function $f(\varepsilon)$ is some simple continuous function of ε such as $\varepsilon^{1/2}$ or $\varepsilon^{3/2}$ and can be defined as:

$$g(\varepsilon) = \frac{1}{e^{(\varepsilon-\mu)/kT} + 1} \quad (29)$$

We have seen already that at $T = 0$ this function $g(\varepsilon)$ is a step function and is defined as:

$$g(\varepsilon) = \begin{cases} 1 & \varepsilon < \mu_0 \\ 0 & \varepsilon > \mu_0 \end{cases} \quad (30)$$

According to Mayer and Mayer [12], also for most metal at $T = 0$, the value of $\mu = \mu_0$ is extremely high, and μ/kT will be of the order of magnitude of 5×10^4 to 5×10^5 K.

Now our task is to show the analysis of evaluating the integral type as it is presented in Eq. (28) given the conditions provided by Ref. [12], which is named under the assumption that $\mu/kT \gg 1$ and their values can be obtained in form of power series for small quantity of kT/μ_0 .

The result will show, a posteriori, that for electrons

in metals this assumption of $\mu/kT \gg 1$ is justifiable up to temperatures above those values at which the metals start melting. Furthermore, in order to integrate the Eq. (28), it will be necessary to play a unique mathematical technique as follows.

Since it can be found that $e^{-\mu/kT} \approx 10^{-40}$, the value of $g(\varepsilon)$ in Eq. (29) reduces to 1 at $\varepsilon = 0$ and decreases monotonously to 0 at $\varepsilon = \infty$ as they are presented here as Eq. (31):

$$g(\varepsilon) = \begin{cases} 1 & \varepsilon = 0 \\ 0 & \varepsilon = \infty \end{cases} \Rightarrow e^{-\mu/kT} \approx 10^{-40} \quad (31)$$

The derivation of $g(\varepsilon)$ as it is given by Eq. (29) designated by $g'(\varepsilon) = dg/d\varepsilon$, is always a negative result, but has one single sharp minimum at $\varepsilon = \mu$, as long as μ is a positive value.

For $\mu/kT \gg 1$, this maximum of $-g'(\varepsilon)$ is very sharp and the function $-g'(\varepsilon)$ is negligibly small for all values of ε differing greatly from $\varepsilon = \mu$. Utilizing technique of partial or part-by-part integration mainly (i.e. $\int u dv = uv - \int v du$ over Eq. (28), may be applied and transformed into an integral over $-F(\varepsilon)g'(\varepsilon)$ (i.e. the $F(\varepsilon)$ being defined as $F(\varepsilon) = \int_0^\varepsilon f(\varepsilon')d\varepsilon'$) as it can be seen here, and because of the form of $-g'(\varepsilon)$, only the values in the neighborhood of $\varepsilon = \mu$ contribute to the integral.

The limits of integration are actually are set from $\varepsilon = 0$ to $\varepsilon = \infty$, but since $-g'(\varepsilon)$ is practically zero for $\varepsilon \leq 0$, no greater error is introduced by changing the limits of integration which can be performed by developing the function $F(\varepsilon)$ as a Taylor's series in powers of $(\varepsilon - \mu)$ about the place of maximum $-g'(\varepsilon)$ [12].

For the purpose of part-by-part integration, we are in need of the first and second derivatives of the function $g(\varepsilon)$ that is presented in Eq. (29) and they are

presented here as Eqs. (32) and (33):

$$g'(\varepsilon) = \frac{dg(\varepsilon)}{d\varepsilon} = -\frac{e^{(\varepsilon-\mu)/kT}}{kT \left[e^{(\varepsilon-\mu)/kT} + 1 \right]^2} \quad (32)$$

and

$$\begin{aligned} g''(\varepsilon) &= \frac{d^2g(\varepsilon)}{d\varepsilon^2} = -\frac{e^{(\varepsilon-\mu)/kT}}{(kT)^2 \left[e^{(\varepsilon-\mu)/kT} + 1 \right]^2} \\ &\quad + \frac{2e^{(\varepsilon-\mu)/kT}}{(kT)^2 \left[e^{(\varepsilon-\mu)/kT} + 1 \right]^3} \\ &= \frac{e^{(\varepsilon-\mu)/kT} \left[e^{(\varepsilon-\mu)/kT} - 1 \right]}{(kT)^2 \left[e^{(\varepsilon-\mu)/kT} + 1 \right]^3} \end{aligned} \quad (33)$$

The first derivative is always negative. The second derivative is zero when the following condition is satisfied as given in Eq. (34):

$$e^{(\varepsilon-\mu)/kT} - 1 = 0$$

for

$$\varepsilon = \mu \quad (34)$$

At $\varepsilon = \mu$, the function $-g'(\varepsilon)$ has a maximum, which is sharper at the lower temperature. The negative of the slope of the original function at this point is greatest.

Using $\varepsilon = \mu$ in Eqs. (29) and (32), we can easily find that the value of the function $g(\varepsilon)$ at this point is given by:

$$g(\varepsilon) = \frac{1}{2} \quad (35)$$

and its derivative namely Eq. (32) is given by:

with

$$g'(\mu) = -\frac{1}{4} \frac{1}{kT} \quad (36)$$

The Napierian logarithmic decrease in $g(\varepsilon)$ with $\ln(\varepsilon)$ is given by Eq. (37) as:

$$-\left(\frac{d \ln g(\varepsilon)}{d \ln(\varepsilon)} \right)_{\varepsilon=\mu} = \frac{1}{2} \frac{\mu}{kT} \quad (37)$$

From this, it can be seen that the relative abruptness of the descent of $g(\varepsilon)$ from almost unity to almost zero increases with the value of μ/kT .

Providing all the above information and equations that we derived, we can generate a set of plots for the Fermis distribution function as it was a derivative for various temperatures as illustrated in Fig. 8. However, note that in Fig. 8, μ should be read in place of μ_0 everywhere.

Note that the function $g(\varepsilon)$ and $g'(\varepsilon)$ are plotted in Fig. 8 for various values of kT .

By partial integration of Eq. (28) of the integral I , we can easily find that:

$$\begin{aligned} I &= \int_0^{\infty} f(\varepsilon)g(\varepsilon)d\varepsilon \\ &= F(\infty)g(\infty) - \int_0^{\infty} F(\varepsilon)g'(\varepsilon)d\varepsilon \end{aligned} \quad (38)$$

where

$$F(\varepsilon) = \int_0^{\varepsilon} f(\varepsilon')d\varepsilon' \quad (39)$$

Analyzing the results of these integral operations, we can easily see that, if $f(\varepsilon)$ is not infinity at $\varepsilon = 0$, then $F(0)$ and the product $F(0)g(0)$ are zero. If $f(\varepsilon)$ does not go exponentially to infinity with ε , the product $F(\infty)g(\infty)$ will be zero since $g(\varepsilon)$ approaches zero as $e^{-\varepsilon/kT}$ with increasing ε .

One may consequently write the result as Eq. (40):

$$I = \int_0^{\infty} f(\varepsilon)g(\varepsilon)d\varepsilon = -\int_0^{\infty} F(\varepsilon)g'(\varepsilon)d\varepsilon \quad (40)$$

We now introduce a new variable that we can transfer to as Eq. (41):

$$x = \frac{\varepsilon - \mu}{kT} \quad (41)$$

and develop the function $F(x)$ as a power series of x as demonstrated in Eq. (42) as:

$$F(x) = \sum_{n=0}^{\infty} \frac{x^n}{n!} F^{(n)}(x=0) \quad (42)$$

where, in the old variable form, we establish Eq. (43):

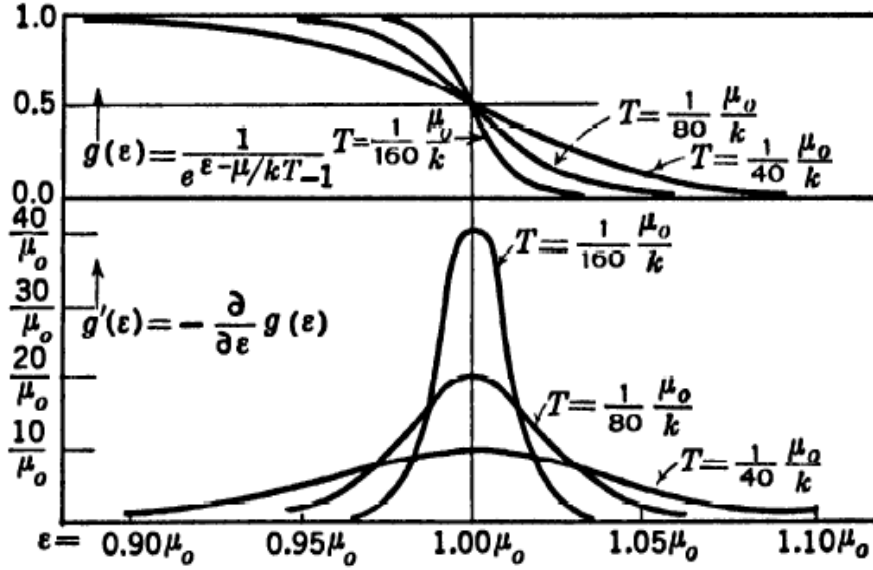


Fig. 8 Fermi distribution function for $g(\epsilon)$ and $g'(\epsilon)$ illustration.

$$F(x=0) = \int_0^\mu f(\epsilon) d\epsilon \quad (43)$$

Thus, we have a new form as Eq. (44) here:

$$\begin{aligned} F^{(n)}(x=0) &= (kT)^n \left[\frac{d^n F(\epsilon)}{d\epsilon^n} \right]_{\epsilon=\mu} \\ &= (kT)^n \left[\frac{d^{n-1} F(\epsilon)}{d\epsilon^{n-1}} \right]_{\epsilon=\mu} \\ &= (kT)^n f^{(n-1)}(\mu) \end{aligned} \quad (44)$$

By substituting Eq. (44) into Eq. (40), we may be able to write Eq. (45) as:

$$\begin{aligned} I &= -F(0) \int_0^\infty g'(\epsilon) d\epsilon \\ &= - \sum_{n=1}^{\infty} \frac{(kT)^n}{n!} f^{(n-1)}(\mu) \int_{x=-\mu/kT}^{\infty} x^n g'(x) dx \end{aligned} \quad (45)$$

The integral of the first term is given as Eq. (46) as:

$$\begin{aligned} - \int_0^\infty g'(\epsilon) d\epsilon &= g(0) - g(\infty) \\ &= \sqrt{1 + e^{-\mu/kT}} \cong 1 \end{aligned} \quad (46)$$

The function $g'(x)$ is obtained by using the expression of Eq. (35) for x in Eq. (32) and write the new equation as Eq. (47) here:

$$\begin{aligned} g'(x) &= - \frac{1}{kT} \frac{e^x}{(e^x - 1)^2} \\ &= - \frac{1}{kT} \frac{1}{(e^x + 1)(e^{-x} + 1)} \end{aligned} \quad (47)$$

The function $g'(x)$ in Eq. (48) is completely symmetrical in x , and can be written as $g'(x) = g'(-x)$. The function approaches zero exponentially as x approaches $-\infty$. If μ/kT is larger, the value of the function is already negligible at the lower limit, $x = -\mu/kT$, of the integral in Eq. (45). No error is introduced and consequently by changing the limits of integration of the terms in the sum of Eq. (45) to $x = -\infty$ and $x = +\infty$.

We must now evaluate the integral of the form as Eq. (48) here:

$$\int_{-\infty}^{+\infty} \left[\frac{x^n}{(e^x + 1)(e^{-x} + 1)} \right] dx \quad (48)$$

From the symmetry of the denominator, it is seen that the integrand is anti-symmetrical in x if n is odd, that is, it changes sign if x is replaced by $-x$ and the integral is therefore zero for odd n . For even values of n , we may integrate from zero to infinity and multiply by 2 and since then the integrand is symmetrical in x .

By developing the following relationship as:

$$\begin{aligned} \frac{1}{(e^x + 1)(e^{-x} + 1)} &= \frac{e^{-x}}{(1 + e^{-x})^2} \\ &= e^{-x} - 2e^{-2x} + 3e^{-3x} - \dots \\ &= -\sum_{m=1}^{\infty} (-1)^m m e^{-mx} \quad (n \text{ even}) \end{aligned} \quad (49)$$

Using Eqs. (46) and (47) with Eqs. (43) and (49), we come to the conclusion as Eq. (50):

$$\begin{cases} I = \int_0^{\infty} f(\varepsilon)g(\varepsilon)d\varepsilon = -\int_0^{\infty} F(\varepsilon)g'(\varepsilon)d\varepsilon \\ = \int_0^{\infty} f(\varepsilon)d\varepsilon - 2\sum_{n=1}^{\infty} (kT)f^{(2n-1)}(\mu)\sum_{m=1}^{\infty} \frac{(-1)^m}{m^{2n}} \\ f^{(2n-1)}(\mu) = \left[\frac{d^{2n-1}f(\varepsilon)}{d\varepsilon^{2n-1}} \right]_{\varepsilon=\mu} \end{cases} \quad (50)$$

The sums occurring have the numerical values as demonstrated in Eq. (51) here:

$$\begin{cases} -\sum_{m=1}^{\infty} \frac{(-1)^m}{m^2} = \frac{\pi^2}{12} \\ \text{and} \\ -\sum_{m=1}^{\infty} \frac{(-1)^m}{m^4} = \frac{7\pi^4}{720} \end{cases} \quad (51)$$

so that

$$\begin{aligned} I &= \int_0^{\infty} \frac{f(\varepsilon)}{e^{(\varepsilon-\mu)/kT} + 1} d\varepsilon \\ &= \int_0^{\infty} f(\varepsilon)d\varepsilon + \frac{\pi^2}{6}(kT)^2 \left(\frac{df}{d\varepsilon} \right)_{\varepsilon=\mu} \\ &\quad + \frac{7\pi^4}{360}(kT) \left(\frac{d^3f}{d\varepsilon^3} \right)_{\varepsilon=\mu} + \dots \end{aligned} \quad (52)$$

Eq. (52) will now be applied to calculate μ . Using Eq. (26), we obtain Eq. (53) as:

$$N = \int_0^{\infty} N(\varepsilon)d\varepsilon = \frac{3N}{2\mu_0^{3/2}} \int_0^{\infty} \frac{\varepsilon^{1/2} d\varepsilon}{e^{(\varepsilon-\mu)/kT} + 1} \quad (53)$$

One finds that $f(\varepsilon) = \varepsilon^{1/2}$ in this problem. The integral $F(\mu)$ is becoming as:

$$\int_0^{\mu} f(\varepsilon)d\varepsilon = \int_0^{\mu} \varepsilon^{1/2} d\varepsilon = \frac{2}{3} \mu^{3/2} \quad (54)$$

The derivatives are as Eq. (55):

$$\begin{cases} \left(\frac{df}{d\varepsilon} \right)_{\varepsilon=\mu} = \frac{1}{2} \mu^{-1/2} \\ \text{and} \\ \left(\frac{d^3f}{d\varepsilon^3} \right)_{\varepsilon=\mu} = \frac{3}{8} \mu^{-5/2} \end{cases} \quad (55)$$

Using Eqs. (54) and (55) with Eq. (52) in Eq. (53), one finds Eq. (56) here as:

$$\left(\frac{\mu}{\mu_0} \right)^{3/2} \left[1 + \frac{\pi^2}{8} \left(\frac{kT}{\mu} \right)^2 + \frac{7\pi^4}{640} \left(\frac{kT}{\mu} \right)^4 + \dots \right] = 1 \quad (56)$$

which determines μ as a function of μ_0 and T .

In order to make the equation explicit in μ , we use the development as Eq. (57) here:

$$\frac{1}{(1+x)^{2/3}} = 1 - \frac{2x}{3} + \frac{5x^2}{9} - \dots \quad (57)$$

which is used to obtain the following for μ as Eq. (58):

$$\mu = \mu_0 \left[1 - \frac{\pi^2}{12} \left(\frac{kT}{\mu} \right)^2 + \frac{\pi^4}{720} \left(\frac{kT}{\mu} \right)^4 + \dots \right] \quad (58)$$

and here $\mu^{-2} = \mu_0^{-2} \left[1 + (\pi^2/6)(kT/\mu_0)^2 \right]$ is substituted in the quadratic term. In the quartic term, which is the last correction, μ_0 is simply substituted for μ . One obtains Eq. (59) for chemical potential μ as:

$$\mu = \mu_0 \left[1 - \frac{\pi^2}{12} \left(\frac{kT}{\mu_0} \right)^2 - \frac{\pi^4}{80} \left(\frac{kT}{\mu_0} \right)^4 + \dots \right] \quad (59)$$

as an equation for μ , it is the chemical potential as we

stated above, in terms of kT and μ_0 .

μ_0 is the chemical potential at $T = 0$ which is given in turn as function of the volume V as it is indicated in Eq. (21).

The energy E may be calculated by using the following relationship as Eq. (60) driven by Eq. (26):

$$E = \int_0^\infty \varepsilon N(\varepsilon) d\varepsilon = \frac{3N}{2\mu_0^{3/2}} \int_0^\infty \frac{\varepsilon^{3/2} d\varepsilon}{e^{(\varepsilon-\mu)/kT} + 1} \quad (60)$$

In the above integral $f(\varepsilon) = \varepsilon^{3/2}$ and then we can write:

$$\left| \begin{aligned} \int_0^\varepsilon f(\varepsilon) d\varepsilon &= \frac{2}{5} \mu^{5/2} \\ \frac{df(\varepsilon)}{d\varepsilon} &= \frac{3}{2} \mu^{1/2} \\ \frac{d^3 f(\varepsilon)}{d\varepsilon^3} &= -\frac{3}{8} \frac{1}{\mu^{3/2}} \end{aligned} \right. \quad (61)$$

so that

$$E = \frac{3}{5} N \mu \left(\frac{\mu}{\mu_0} \right)^{3/2} \left[1 + \frac{5\pi^2}{8} \left(\frac{kT}{\mu} \right)^2 - \frac{7\pi^4}{384} \left(\frac{kT}{\mu} \right)^4 + \dots \right] \quad (62)$$

is obtained.

By using Eq. (59) to replace μ with μ_0 , one can find out Eq. (63) for the energy E as:

$$E = \frac{3}{5} N \mu_0 \left[1 + \frac{5\pi^2}{12} \left(\frac{kT}{\mu_0} \right)^2 - \frac{\pi^4}{16} \left(\frac{kT}{\mu_0} \right)^4 + \dots \right] \quad (63)$$

7. The Thermodynamic Functions of a Degenerate Fermi-Dirac Gas

The chemical potential μ as illustrated in Eq. (59) and the energy E from Eq. (63) for the generate Fermi-Dirac gas have been derived as a power series of the temperature T in terms of μ_0 as well volume V as Eq. (21).

Eq. (63), giving energy E as a function of

temperature T and volume V , can be obtained as:

$$E = \frac{3}{5} N \mu_0 \left[1 + \frac{5\pi^2}{12} \left(\frac{kT}{\mu_0} \right)^2 - \frac{\pi^4}{16} \left(\frac{kT}{\mu_0} \right)^4 + \dots \right] = N \mu_0 \left[\frac{3}{5} + \frac{\pi^2}{4} \left(\frac{kT}{\mu_0} \right)^2 - \frac{3\pi^4}{80} \left(\frac{kT}{\mu_0} \right)^4 + \dots \right] \quad (64)$$

With help from Eq. (21), we can then write the following set of Eq. (65) as:

$$\mu_0 = \frac{h^2}{8m} \left(\frac{3N}{\pi V} \right)^{2/3} \quad \frac{d\mu_0}{dV} = -\frac{2\mu_0}{3V} \quad (65)$$

which would be sufficient to permit the calculation of all other thermodynamic functions at entropy of $S = 0$ at the temperature $T = 0$. [12]

The heat capacity at constant volume C_V is found by direct differentiation of results of Eq. (64). Then we can write:

$$C_V = Nk \frac{\pi^2 kT}{2 \mu_0} \left[1 - \frac{3\pi^2}{10} \left(\frac{kT}{\mu_0} \right)^2 + \dots \right] \quad (66)$$

The entropy S may be obtained by integration of $\int_0^T (C_V/T) dT$, thus we can write:

$$S = \int_0^T \frac{C_V}{T} dT = Nk \frac{\pi^2 kT}{2 \mu_0} \left[1 - \frac{\pi^2}{10} \left(\frac{kT}{\mu_0} \right)^2 + \dots \right] = \frac{N\mu_0}{T} \left[\frac{\pi^2}{2} \left(\frac{kT}{\mu_0} \right)^2 - \frac{\pi^4}{20} \left(\frac{kT}{\mu_0} \right)^4 + \dots \right] \quad (67)$$

The work function of $A = E - TS$ is from Eqs. (64) and (67) in the following form of Eq. (68):

$$A = N \mu_0 \left[\frac{3}{5} - \frac{\pi^2}{4} \left(\frac{kT}{\mu_0} \right)^2 + \frac{\pi^4}{80} \left(\frac{kT}{\mu_0} \right)^4 - \dots \right] = \frac{3}{5} N \mu_0 \left[1 - \frac{5\pi^2}{12} \left(\frac{kT}{\mu_0} \right)^2 + \frac{\pi^4}{48} \left(\frac{kT}{\mu_0} \right)^4 - \dots \right]$$

(68)

The pressure P is given by $-(\partial A/\partial V)_T$ and with help from Eq. (65) being substituted in Eq. (68), one can get the result that is shown in Eq. (4), and that is the result we are looking for, thus we may establish the Eq. (69) as:

$$\begin{aligned}
 P &= \frac{N\mu_0}{V} \left[\frac{2}{5} + \frac{\pi^2}{6} \left(\frac{kT}{\mu_0} \right)^2 - \frac{\pi^4}{40} \left(\frac{kT}{\mu_0} \right)^4 + \dots \right] \\
 &= \frac{3}{5} \frac{5}{3} \left(\frac{N}{V} \right) \mu_0 \left[\frac{2}{5} + \frac{\pi^2}{6} \left(\frac{kT}{\mu_0} \right)^2 - \frac{\pi^4}{40} \left(\frac{kT}{\mu_0} \right)^4 + \dots \right] \\
 &= \frac{2}{3} \left(\frac{N}{V} \right) \mu_0 \left[\frac{3}{5} + \frac{\pi^2}{4} \left(\frac{kT}{\varepsilon_F} \right)^2 - \frac{3\pi^4}{80} \left(\frac{kT}{\varepsilon_F} \right)^4 + \dots \right] \\
 &= \frac{2}{3} \frac{E}{V}
 \end{aligned} \tag{69}$$

The equation $PV = 2E/3V$ is found at $T = 0$ Kelvin, and Eq. (70) is seen to be independent of temperature T [12].

$$P_0 = -\frac{\partial E_0}{\partial V} = -\frac{3}{5} N \frac{\partial \mu_0}{\partial V} = \frac{2}{5} \frac{N}{V} \mu_0 = \frac{2}{3} \frac{E_0}{V} \tag{70}$$

We can also derive the heat content with help of $H = E + PV$ and it accordingly yields Eq. (71) as:

$$\begin{aligned}
 H &= \frac{5}{3} E \\
 &= N\mu_0 \left[1 + \frac{5\pi^2}{12} \left(\frac{kT}{\mu_0} \right)^2 - \frac{\pi^4}{16} \left(\frac{kT}{\mu_0} \right)^4 + \dots \right]
 \end{aligned} \tag{71}$$

Finally, forming $F = H - TS$ would provide us with Eq. (72) as:

$$F = N\mu_0 \left[1 - \frac{\pi^2}{12} \left(\frac{kT}{\mu_0} \right)^2 - \frac{\pi^4}{80} \left(\frac{kT}{\mu_0} \right)^4 + \dots \right] \tag{72}$$

which is, of course, can be seen to be as $N\mu$ by comparison with Eq. (59).

All the above equation for degenerate Fermi-Dirac gas was derived based on $kT \ll \varepsilon_F$, which is an indication of strongly degenerate gas case.

It is to be noted that in all the equations for the thermodynamic properties of the gas the temperature-dependent part occurs as kT/μ_0 . Since μ_0/k is about 10^5 K for the molar volumes of an electron in metals, kT/μ_0 is about 10^{-3} K to 10^{-2} K for ordinary temperatures. The thermodynamic functions of degenerate gas, at the concentrations considered, do not depend greatly on temperature T . In particular, the heat capacity is almost negligible compared to that due to the vibrations of the ions up to considerable temperature.

In the case of $kT \gg \varepsilon_F$, which is considered to a non-degenerate gas, the considerations will be very similar to the corresponding case discussed in Eliezer, et. al. [26] for a Bose-Einstein gas except that we would have to use the following expansion as illustrated in Eq. (73) [26]:

$$\begin{aligned}
 g_n(y) &\equiv \frac{1}{\Gamma(n)} \int_0^\infty \frac{x^{n-1} dx}{(1/y)e^x + 1} \\
 &= \frac{1}{\Gamma} \int_0^\infty ye^{-x} (1 + ye^{-x})^{-1} x^{n-1} dx \\
 &= \frac{1}{\Gamma} \int_0^\infty ye^{-x} [1 - ye^{-x} + y^2 e^{-2x} + \dots] x^{n-1} dx \\
 &= y - \frac{y^2}{2^n} + \frac{y^3}{3^n} - \dots
 \end{aligned} \tag{73}$$

The final results for the various thermodynamic functions have already been given in the book Eliezer et. al. [26], chapter (5.64) and (5.68); the lower signs correspond to Fermi-Dirac statistics and for an electron gas $G=2$.

With this, we come to the conclusion of the short review.

8. Conclusion

In conclusion, we are hoping that we have managed to bring the functions of a degenerate Fermi-Dirac gas

together as a short review via statistical mechanics approach and readers are no longer need to search for them and their related derivation by looking all over the textbooks as well as internet these days, such as Wikipedia.org or any other resource.

References

- [1] Zohuri, B. 2017. *Inertial Confinement Fusion Driven Thermonuclear Energy*. Springer International Publishing.
- [2] Nuckolls, J., Wood, L., Thiessen, A., and Zimmerman, G. 1972. "Laser Compression of Matter to Super-high Densities: Thermonuclear (CTR) Applications." *Nature* 239 (5368): 139-42.
- [3] Guderley K G. 1942. "Starke kugelige und zylindrische verdichtungsstosse in der nahe des kugelmittelpunktes bzw. der zylinderachse." *Luftfahrtforschung* 19: 302.
- [4] Behgounia, F., Nezam, Z. Z., and Zohuri, B. 2020. "Dimensional Analysis and Similarity Method Driving Self-similar Solutions of the First and Second Kind Inducing Energy." *Journal of Energy and Power Engineering* 14: 233-50. doi:10.17265/1934-8975/2020.07.003
- [5] Zohuri, B. 2015. *Dimensional Analysis and Self-similarity Methods for Engineers and Scientists*. Springer Publishing Company.
- [6] Zohuri, B. 2017. *Dimensional Analysis Beyond the Pi Theorem*. Springer International Publishing.
- [7] Lawson, J. D. 1957. "Some Criteria for a Power Producing Thermonuclear Reactor." *Proc. Phys. Soc. (Lond.) B70* (1): 6.
- [8] Gough, W. C., and Eastlund, B. J. 1971. "The Prospects of Fusion Power." *Scientific American* 224 (2): 50-67.
- [9] Schwarzschild, M. 1965. *Structure and Evolution of the Stars*. New York: Dover, p206.
- [10] Chandrasekhar, S. 1938. *Stellar Structure*. Chicago: University of Chicago Press, p427.
- [11] Landau, L., and Lifshitz, E. 1969. *Statistical Physics*, ch. 5. Addison/Wesley, Reading.
- [12] Mayer, J., and Mayer, M. 1940. *Statistical Mechanics*. Wiley, p385.
- [13] Wikipedia. "Electron Degeneracy Pressure." Accessed January 22, 2021. https://en.wikipedia.org/wiki/Electron_degeneracy_pressure.
- [14] Wikipedia. "Degenerate Energy Levels." Accessed January 22, 2021. https://en.wikipedia.org/wiki/Degenerate_energy_levels.
- [15] Dyson, F. J., and Lenard, A. 1967. "Stability of Matter I." *J. Math. Phys.* 8 (3): 423-34. Bibcode:1967JMP....8..423D. doi:10.1063/1.1705209.
- [16] Lenard, A., and Dyson, F. J. 1968. "Stability of Matter II." *J. Math. Phys.* 9 (5): 698-711. Bibcode:1968JMP....9..698L. doi:10.1063/1.1664631.
- [17] Dyson, F. J. 1967. "Ground-State Energy of a Finite System of Charged Particles." *J. Math. Phys.* 8 (8): 1538-45. Bibcode:1967JMP....8.1538D. doi:10.1063/1.1705389.
- [18] Wikipedia. "White Dwarf." Accessed January 22, 2021. https://en.wikipedia.org/wiki/White_dwarf.
- [19] Griffiths, D. J. 2005. *Introduction to Quantum Mechanics*. Second Edition. London, UK: Prentice Hall.
- [20] Mazzali, P. A., Röpke, F. K., Benetti, S., and Hillebrandt, W. 2007. "A Common Explosion Mechanism for Type Ia Supernovae." *Science* 315 (5813): 825-8. arXiv:astro-ph/0702351. Bibcode:2007Sci...315..825M. doi:10.1126/science.1136259. PMID1728999.
- [21] Timmes, F. X., Woosley, S. E., and Weaver, T. A. 1996. "The Neutron Star and Black Hole Initial Mass Function." *Astrophysical Journal* 457: 834-43. arXiv:astro-ph/9510136. Bibcode:1996ApJ...457..834T. doi:10.1086/176778.
- [22] Lieb, E. H., and Yau, H. T. 1987. "A Rigorous Examination of the Chandrasekhar Theory of Stellar Collapse." *Astrophysical Journal* 323: 140-4. Bibcode:1987ApJ...323..140L. doi:10.1086/165813.
- [23] Chandrasekhar, S. 1931. "The Density of White Dwarf Stars." *The London, Edinburgh, and Dublin Philosophical Magazine and Journal of Science* 11 (70): 592-6. doi:10.1080/14786443109461710.
- [24] Chandrasekhar, S. 1935. "The Highly Collapsed Configurations of a Stellar Mass (Second Paper)." *Monthly Notices of the Royal Astronomical Society* 95 (3): 207-25. Bibcode:1935MNRAS..95..207C. doi:10.1093/mnras/95.3.207.
- [25] Ochsenbein, F., and Centre de Données astronomiques de Strasbourg (CDS). 2000. "Standards for Astronomical Catalogues, Version 2.0, Section 3.2.2." Accessed January 12, 2020. <http://vizier.u-strasbg.fr/vizier/doc/catstd.pdf>.
- [26] Eliezer, S., Ghatik, A., and Hora. H. 1986. *Fundamentals of Equations of State*. New Jersey: World Scientific Publishing Company.